C−C and C−H Bond Activation at Ruthenium(II): The Stepwise Degradation of a Neopentyl Ligand to a Trimethylenemethane Ligand

Kristopher McNeill, Richard A. Andersen,* and Robert G. Bergman*

Contribution from the Materials and Chemical Sciences Division, Lawrence Berkeley Laboratory, and the Department of Chemistry, University of California, Berkeley, California 94720

Received June 26, 1997[⊗]

Abstract: Ruthenacyclobutane complexes $(SiP_3)(PMe_3)Ru(CH_2EMe_2CH_2)$ $(SiP_3 = MeSi(CH_2PMe_2)_3$; **1**, E = C; **2**, E = Si) were synthesized from $(SiP_3)(PMe_3)RuCl_2$ (**3**) and 2 equiv of the Grignard reagents, Me_3ECH_2MgCl. Metallacycle **1** was found to reversibly interconvert with the allyl complex $(SiP_3)Ru(Me)(\eta^3\text{-}CH_2CMeCH_2)$ (**4**) and PMe_3 when heated above 75 °C. From the results of kinetic studies and thermolysis of labeled material, the interconversion is proposed to take place by reversible β-methyl elimination/insertion. Conversion of **1** to **4** is an endothermic process ($\Delta H° = 14.3 \pm 1.1$ kcal mol^{-1}), but it is entropically favorable ($\Delta S° = 40.9 \pm 2.8$ cal K^{-1} mol^{-1}) due to the loss of the PMe_3 ligand. Activation parameters for the β-insertion were determined to be $\Delta H^\ddagger = 26.0 \pm 1.2$ kcal mol^{-1} and $\Delta S^\ddagger = -10.5 \pm 0.9$ cal K^{-1} mol^{-1}. Allyl complex **4** has been isolated as a mixture of isomers (7:1 *endo:exo*). The mechanism of interconversion of $\mathbf{4_{endo}}$ and $\mathbf{4_{exo}}$ was determined by $^1H\{^{31}P\}$ NMR spectroscopy (EXSY) to be a process involving a stereochemically rigid, square-pyramidal η^1-intermediate. Thermolysis of **4** leads to loss of CH_4 and the production of the trimethylenemethane complex $(SiP_3)Ru(\eta^4\text{-}C(CH_2)_3)$ (**7**). The solid state structures of **1** and **7** were determined by X-ray diffraction.

Introduction

Transition metals have been proposed to play important roles in the breakdown of hydrocarbons in processes such as coal liquefaction,[1,2] petroleum cracking,[3−5] microbial (enzymatic) degradation of organic matter,[6−9] and the geochemical formation of natural gas.[10−12] However, understanding of metal-mediated hydrocarbon degradation processes has been limited, in part due to the relative rarity of C−C activation reactions performed with well-defined metal complexes.[13] One class of reactions that has become increasingly recognized as a viable C−C cleavage process is β-alkyl elimination (eq 1).[14−37] Over the past 15

years, observations of β-alkyl elimination have been documented in a number of early transition metal complexes[14−26] and a handful of late metal systems.[27−35] In a previous communication,

$$(1)$$
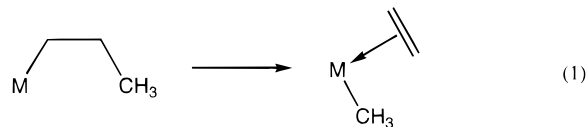
we reported our discovery of the first direct observation of reversible β-methyl elimination/migratory insertion.[33] In this contribution, we provide a more complete mechanistic picture of this C−C bond cleavage and show that it is the central process in a larger scheme: the degradation of a neopentyl complex to a trimethylenemethane complex via metallacyclobutane and allyl intermediates.

[⊗] Abstract published in *Advance ACS Abstracts,* November 1, 1997.

(1) Cheung, T.-K.; d'Itri, J. L.; Lange, F. C.; Gates, B. C. *Catal. Lett.* **1995,** *31,* 153.

(2) Cheung, T.-K.; d'Itri, J. L.; Gates, B. C. *J. Catalysis* **1995,** *153,* 344.

(3) Farcasiu, M.; Smith, C. *Energy Fuels* **1991,** *5,* 83.

(4) Walter, T. D.; Casey, S. M.; Klein, M. T.; Foley, H. C. *Energy Fuels* **1994,** *8,* 470.

(5) Walter, T. D.; Klein, M. T. *Energy Fuels* **1995,** *9,* 1058.

(6) Bragg, J. R.; Prince, R. C.; Harner, E. J.; Atlas, R. M. *Nature* **1994,** *368,* 413.

(7) Atlas, R. M. *Petroleum Microbiology*; Atlas, R. M., Ed.; Macmillan: New York, 1984; p 692.

(8) Baker, K. H.; Herson, D. S. *Geomicrobiol. J.* **1990,** *8,* 133.

(9) Grbic-Galic, D. *Geomicrobiol. J.* **1990,** *8,* 167.

(10) Mango, F. D.; Hightower, J. W.; James, A. T. *Nature* **1994,** *368,* 536.

(11) Mango, F. D. *Org. Geochem.* **1996,** *24,* 977.

(12) Price, L. C.; Schoell, M. *Nature* **1995,** *378,* 368.

(13) Crabtree, R. H. *Chem. Rev.* **1985,** *85,* 245.

(14) Corker, J.; Lefebvre, F.; Lécuyer, C.; Dufaud, V.; Quignard, F.; Choplin, A.; Evans, J.; Basset, J.-M. *Science* **1996,** *271,* 966.

(15) Watson, P. L.; Parshall, G. W. *Acc. Chem. Res.* **1985,** *18,* 51.

(16) Watson, P. L.; Roe, D. C. *J. Am. Chem. Soc.* **1982,** *104,* 6471.

(17) Bunel, E.; Burger, B. J.; Bercaw, J. E. *J. Am. Chem. Soc.* **1988,** *110,* 976.

(18) Bercaw, J. E. *Pure Appl. Chem.* **1990,** *62,* 1151.

(19) Hajela, S.; Bercaw, J. E. *Organometallics* **1994,** *11,* 362.

(20) Eshuis, J. J. W.; Tan, Y. Y.; Teuben, J. H.; Renkema, J. *J. Mol. Catal.* **1990,** *62,* 277.

(21) Eshuis, J. J. W.; Tan, Y. Y.; Meetsma, A.; Teuben, J. H.; Renkema, J.; Evens, G. G. *Organometallics* **1992,** *11,* 362.

(22) Kesti, M. R.; Waymouth, R. M. *J. Am. Chem. Soc.* **1992,** *114,* 3565.

(23) Resconi, L.; Piemontesi, F.; Franciscono, G.; Abis, L.; Fiorani, T. *J. Am. Chem. Soc.* **1992,** *114,* 1025.

(24) Yang, X.; Jia, L.; Marks, T. J. *J. Am. Chem. Soc.* **1993,** *115,* 3392.

(25) Horton, A. D. *Organometallics* **1996,** *15,* 2675.

(26) Etienne, M.; Mathieu, R.; Donnadieu, B. *J. Am. Chem. Soc.* **1997,** *119,* 3218.

(27) Flood, T. C.; Bitler, S. P. *J. Am. Chem. Soc.* **1984,** *106,* 6076.

(28) Flood, T. C.; Statler, J. A. *Organometallics* **1984,** *3,* 1795.

(29) Ermer, S. P.; Struck, G. E.; Bitler, S. P.; Richards, R.; Bau, R.; Flood, T. C. *Organometallics* **1993,** *12,* 2634.

(30) Hartwig, J. F.; Bergman, R. G.; Andersen, R. A. *Organometallics* **1991,** *10,* 3344.

(31) Thomson, S. K.; Young, G. B. *Organometallics* **1989,** *8,* 2068.

(32) Ankianiec, B. C.; Christou, V.; Hardy, D. T.; Thompson, S. K.; Young, G. B. *J. Am. Chem. Soc.* **1994,** *116,* 9963.
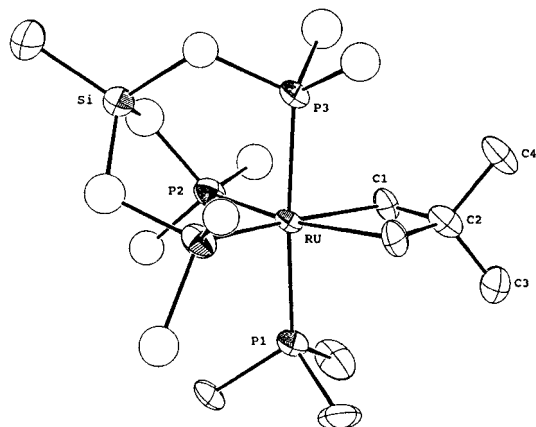
(33) McNeill, K.; Andersen, R. A.; Bergman, R. G. *J. Am. Chem. Soc.* **1995,** *117,* 3625.

(34) Jun, C.-H.; Kang, J.-B.; Lim, Y.-G. *Tetrahedron Lett.* **1995,** *36,* 277.

(35) Jun, C.-H. *Organometallics* **1996,** *15,* 895.

(36) Observation of β-methyl elimination in the gas phase: Karrass, S.; Schwartz, H. *Organometallics* **1990,** *9,* 2409.

(37) Karrass, S.; Schwartz, H. *Organometallics* **1990,** *9,* 2034.

C−C and C−H Bond Activation at Ruthenium(II)

J. Am. Chem. Soc., Vol. 119, No. 46, 1997 11245

Figure 1. ORTEP diagram of **1**. Selected bond distances (Å) and angles (deg): Ru−C1 = 2.180(10), Ru−P1 = 2.339(4), Ru−P2 = 2.307(3), Ru−P3 = 2.343(4), C1−C2 = 1.552(14), C2−C3 = 1.524(22), C2−C4 = 1.552(21), C1−Ru−C1 = 66.4(6), Ru−C1−C2 = 96.6(7), C1−C2−C1 = 100.5(11), P1−Ru−P2 = 93.82(10), P1−Ru−P3 = 175.92(16), P2−Ru−P2 = 97.24(16), P2−Ru−P3 = 88.87(11).

Scheme 1
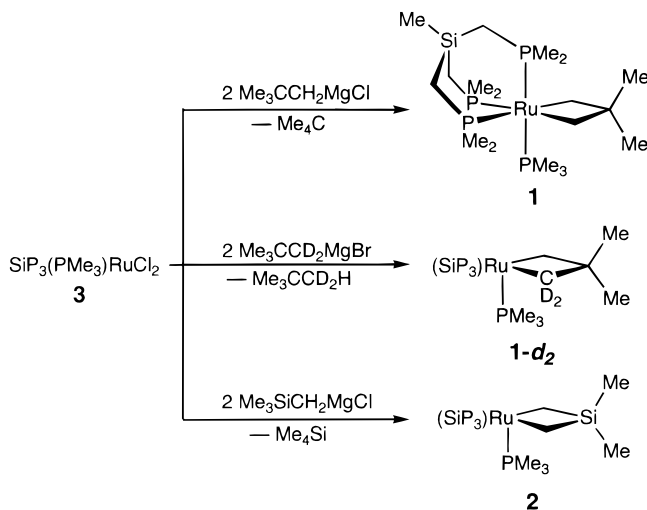
Results

Synthesis of Metallacyclobutanes. The metallacyclobutanes $(SiP_3)(PMe_3)Ru(CH_2CMe_2CH_2)$ (**1**), $(SiP_3)(PMe_3)Ru(CD_2CMe_2-CH_2)$ (**1-d_2**), and $(SiP_3)(PMe_3)Ru(CH_2SiMe_2CH_2)$ (**2**) ($SiP_3 = MeSi(CH_2PMe_2)_3$) were synthesized by treatment of $(SiP_3)-(PMe_3)RuCl_2$ (**3**) with the appropriate Grignard reagent (Scheme 1). In each case, clean cyclometalation to give the metallacycle was observed by ^1H and $^{31}P\{^1H\}$ NMR spectroscopy. The metallacycles were isolated in good yields and purified by crystallization from pentane or hexane solvents. When the reactions were followed by NMR spectroscopy, the metallacyclic complexes and the corresponding alkanes (CMe_4, $SiMe_4$) were the only products observed. The solid-state structure of **1** was determined by a single-crystal X-ray diffraction study. Crystallographic disorder of the tripodal phosphine ligand was observed, and was successfully modeled as 1:1 occupancy of the two twist-related conformations of the SiP_3 ligand. The four-membered ring is well-ordered and is found to be planar with no close contacts between the metal center and the ring-bound methyl groups. An ORTEP diagram of **1** is shown in Figure 1.

Complex **1-d_2** was examined by ^1H and $^2H\{^1H\}$ NMR and was found to have deuterium incorporated into the α-position of the metallacycle and no other site. The deuteration was judged to be 83% on the basis of $^1H\{^{31}P\}$ NMR integration. Mass spectrometric studies confirmed increased mass in many

of the daughter ions upon deuteration, but because the parent ion was not detected the extent of deuterium incorporation was not quantified by this method.

Interconversion of 1 and $(SiP_3)Ru(Me)(\eta^3\text{-}CH_2CMeCH_2)$ (4). Thermolysis of **1** produces $(SiP_3)Ru(Me)(\eta^3\text{-}CH_2CMeCH_2)$ (**4**) in >98% yield as measured by ^1H NMR spectroscopy (integration against internal standard) (eq 2). Complex **4** was
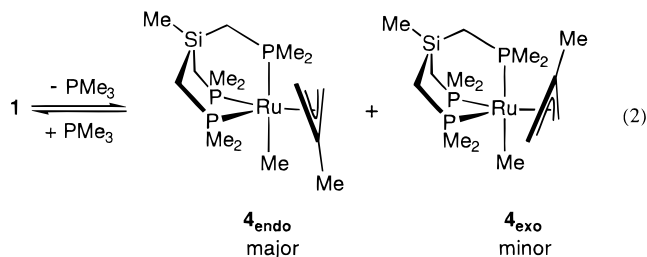
isolated as a mixture of *endo* and *exo* isomers (7:1, *endo:exo*) in 42% yield after crystallization from $(Me_3Si)_2O$. Additional confirmation of the structure of the thermolysis product was provided by the independent preparation from $(SiP_3)(PMe_3)-Ru(Me)(Cl)$, **6**, and $CH_3C(CH_2)CH_2MgBr$ (eq 3).
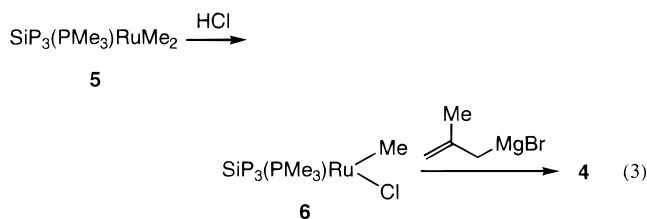
The structures of isomers **4$_{endo}$** and **4$_{exo}$** were determined by a variety of NMR experiments which allowed unambiguous assignments and determination of the *endo:exo* ratio. The process of identification first involved assignment of all of the resonances in the ^1H, $^{31}P\{^1H\}$, and $^{13}C\{^1H\}$ one-dimensional NMR spectra to the major and minor isomers. Correlation of resonances in these spectra was made by $^1H/^{13}C\{^1H\}$ and $^1H-\{^{31}P\}/^{31}P\{^1H\}$ HMQC two-dimensional experiments. On the basis of these correlations and the stereochemical relationship of the phosphorus nuclei apparent from the characteristic *trans* and *cis J* coupling values, most of the assignments could be made. Four stereochemical features remained ambiguous after these experiments: orientation of the allyl ligand in each isomer, assignment of the ^1H resonances for the *syn* and *anti* protons of the allyl ligand, assignment of the SiP_3 ligand Me_B and Me_C resonances, and assignment of the two ^1H resonances of the SiP_3 methylene units that are *trans* to the allyl ligand (see Figure 2). A $^1H\{^{31}P\}$ NOESY experiment allowed assignment of these remaining features. The major isomer was found to be the *endo* isomer with the room temperature ratio being approximately 7:1 *endo:exo*.

The silaruthenacyclobutane, **2**, was not observed to undergo similar rearrangement. When **2** was heated to 105 °C for 2 h in C_6D_6, decomposition to several unidentified products was observed.

Compound **4** is the product of a formal β-methyl transfer reaction, and a study of the mechanism of its formation was undertaken. The reversibility of the **1−4** interconversion was established initially by observing that conversion of **1** to **4** was dependent on the phosphine concentration. This was further demonstrated by reconversion of an isolated sample of **4** to an equilibrium mixture of **1** and **4** by the addition of PMe_3. Thermodynamic quantities for the interconversion were determined from the temperature dependence of the equilibrium
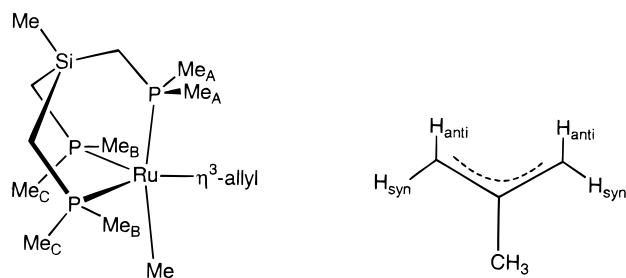
Figure 2. Labeling scheme employed for complex **4**.

Table 1. Rate and Equilibrium Data for the Conversion of **1** to **4** in Toluene-d_8

entry	[PMe$_3$] (mol/L)	T (±0.2 °C)	$10^4 k_{obs}$ (s^{-1})	$10^4 k_{-2}$ (s^{-1})	K_{eq}
1	0.12(3)	96.0	2.69(4)	0.29(2)	0.97(1)
2	0.19(3)	96.0	1.66(6)	0.22(7)	1.19(9)
3	0.25(3)	96.0	1.34(3)	0.22(1)	1.33(3)
4	0.37(3)	96.0	1.08(4)	0.24(2)	1.27(3)
5	0.46(3)	96.0	0.860(9)	0.18(4)	1.70(5)
6	0.98(3)	96.0	0.577(17)	0.18(8)	1.21(4)
7	1.06(3)	96.0	0.503(15)	0.156(5)	2.36(4)
8	1.90(4)	96.0	0.343(26)	0.18(1)	1.64(6)
9	0.49(2)	73.6	0.0376(29)	0.015(2)	0.75(5)
10	0.49(2)	90.5	0.512(30)	0.085(11)	2.45(23)
11	0.49(2)	105.1	2.96(16)	0.308(18)	4.21(9)
12	0.49(2)	117.3	21.9(8)	1.24(17)	8.16(9)
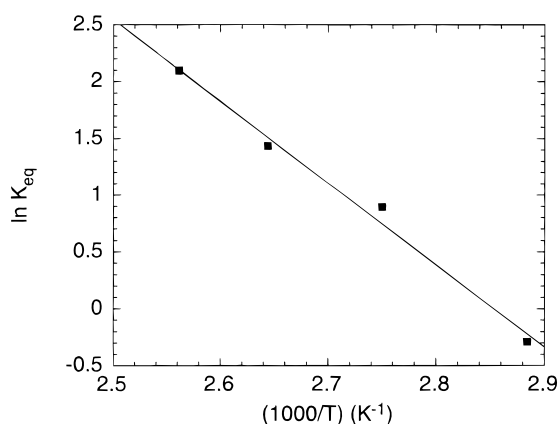
Figure 3. Temperature dependence of K_{eq} (73.6 < T < 117.3 °C).
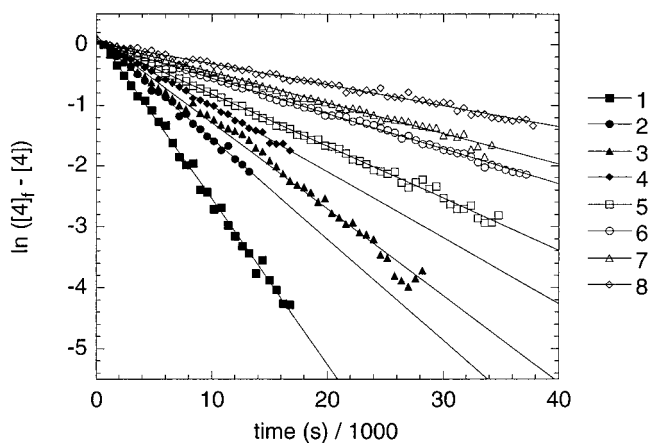

Figure 4. Kinetic traces for the conversion of **1** to **4** (96.0 °C) at various PMe$_3$ concentrations. The legend refers to numbered entries in Table 1.

constant (73.6 to 117.3 °C, Figure 3): As written in eq 2, $\Delta G°_{rxn}$(363.7 K, 1 M PMe$_3$) = −1.16 ± 0.07 kcal mol^{-1}, $\Delta H°_{rxn}$(1 M PMe$_3$) = 14.3 ± 1.1 kcal mol^{-1}, and $\Delta S°_{rxn}$(1 M PMe$_3$) = 40.9 ± 2.8 cal K^{-1} mol^{-1}.
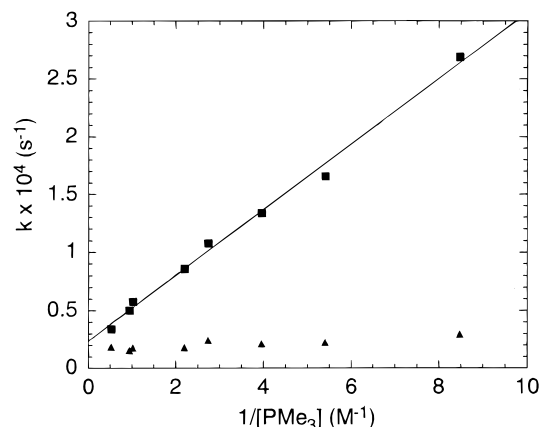
Figure 5. Phosphine concentration dependence on k_{obs}. Rate constants versus [PMe$_3$]$^{-1}$: (■) k_{obs}, (▲) k_{-2} calculated from each run.
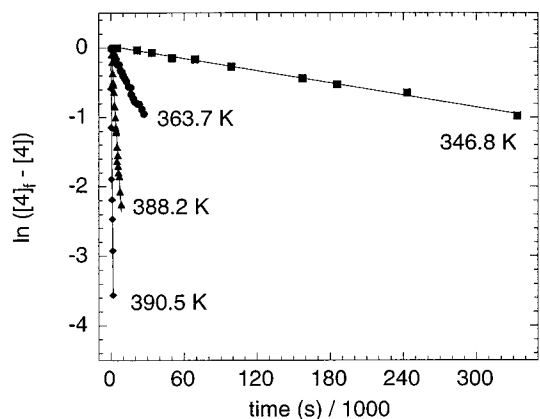

Figure 6. Kinetic traces for the conversion of **1** to **4** (0.49 M PMe$_3$) at various temperatures.

A kinetic study was performed with ^{1}H{^{31}P}NMR spectroscopy to monitor the progress of the forward reaction (eq 2, Table 1). The reactions were performed in the presence of excess PMe$_3$, which simplified the kinetic behavior of the system. Under these conditions, pseudo-first-order rate constants for the disappearance of **1** and appearance of **4** were obtained (Figure 4). In each case the values for the appearance and disappearance were equivalent within error. The reaction rate was found to be inversely proportional to the concentration of PMe$_3$, converging to (2.4 ± 0.4) × 10^{-5} s^{-1} at high [PMe$_3$] (Figure 5). The temperature dependence of the reaction rate was measured (345.8 K < T < 390.5 K, Figure 6), making possible calculation of $\Delta G^{\ddagger}$, $\Delta H^{\ddagger}$, and $\Delta S^{\ddagger}$ for the interconversion process (see Discussion). The rate of PMe$_3$ exchange was measured by treating **1** with an excess of PMe$_3$-d_9 (eq 4). First-order behavior was observed for the approach to equilibrium (Figure 7).[38]
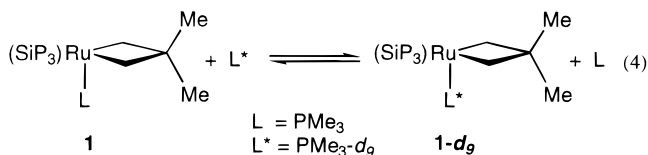

A labeling experiment was performed to help elucidate the mechanism of the overall β-methyl transfer. Thermolysis of **1-d_2** yields one isotopomer of each of the *exo* and *endo* allyl species, (SiP$_3$)Ru(η^3-CD$_2$CMeCH$_2$)(CH$_3$), **4-d_2**, as confirmed by NMR spectroscopy (^{1}H, ^{2}H{^{1}H}, and ^{13}C{^{1}H}) and mass

(38) Espenson, J. H. *Chemical Kinetics and Reaction Mechanisms*; McGraw-Hill, Inc.: New York, 1981.
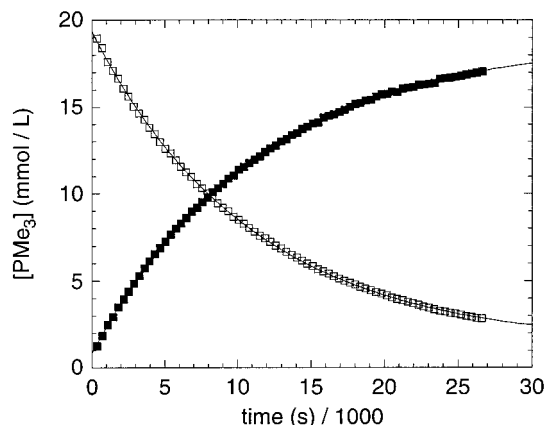
Figure 7. Conversion of **1** to **1-d_9** by exchange of PMe$_3$ (363.0 K) monitored by ^{1}H{^{31}P} NMR spectroscopy: (■) free PMe$_3$; (□) bound PMe$_3$ in complex **1**. The solid line corresponds to the curve fit.

spectrometry (eq 5). No ^{2}H was detected in the Ru-bound methyl group (see Discussion).
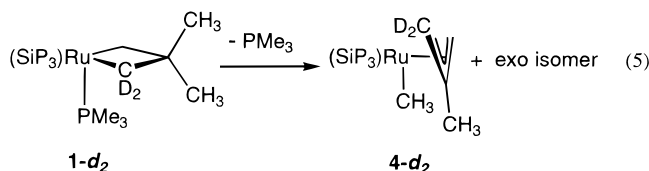
NMR Study of the Interconversion of 4$_{endo}$ and 4$_{exo}$. As has been mentioned previously, complex **4** was observed to be a mixture of the *endo* and *exo* isomers. It became clear from preliminary variable-temperature NMR spectroscopy experiments that the interconversion of these was facile, and the observed ratio of **4$_{endo}$** and **4$_{exo}$** (ca. 7:1 at 20 °C) represented the thermodynamic ratio. To probe the dynamic exchange mechanism between the *endo* and *exo* isomers of **4**, ^{1}H{^{31}P} EXSY NMR spectra were acquired at 54.9 °C at various mixing times (10, 20, 40, and 100 ms). The data clearly show exchange between ^{1}H sites of the allyl ligand of the major and minor isomer (Figure 8). The experiments at different mixing times show the development of label exchange with time, such that at 10 ms there is very little exchange and at 100 ms there is exchange among all of the allyl sites. The early experiments (10, 20, and 40 ms) are particularly clear in showing that *inter*isomer exchange is *faster* than *intra*isomer exchange.

At early mixing times, there is exchange between a given ^{1}H site with *both* of the allyl ^{1}H sites of the *other* isomer and *no* exchange within sites of the *same* isomer (see Figure 2 for labeling scheme). For example, the protons occupying *anti* sites of the major isomer (δ 2.24) are exchanging with protons at the *anti* and *syn* sites of the minor isomer (δ 2.63, 1.73) and not with protons at the *syn* site of the major isomer (δ 1.49). The EXSY data also indicate that the three P atoms of the SiP$_3$ ligand and the methyl ligand maintain their stereochemical relationship with one another during the major—minor interconversion; magnetization is transferred from the Me$_A$ sites of the major isomer (δ 0.85) to Me$_A$ sites of the minor isomer (δ 0.92) and not the Me$_B$ or Me$_C$ sites of the minor isomer (δ 1.34, 1.31).
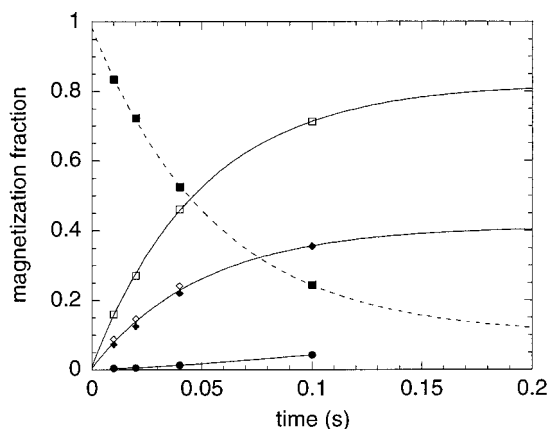
Figure 10 shows the evolution of magnetization transfer with time at 59.9 °C. At $t = 0$ s, the magnetization starts with the minor isomer *anti* protons. The minor isomer converts to the major isomer transferring the magnetization to the *anti* and *syn* sites of the major isomer. After some of the labeled major isomer has built up in solution (ca. 40—100 ms), magnetization transfer back to the minor isomer (in the *syn* site) is observed. From these kinetic traces, the forward and backward rate can
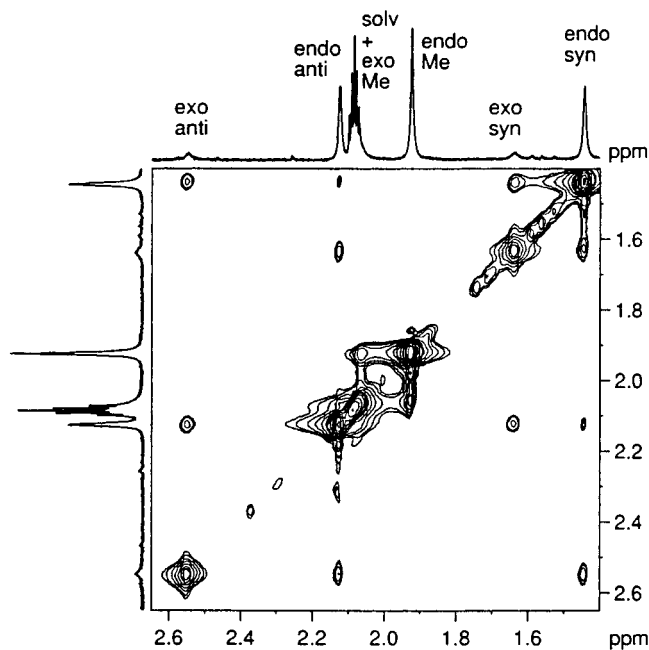
Figure 8. ^{1}H{^{31}P} EXSY spectrum of **4** at 54.9 °C with a 20 ms mixing time.
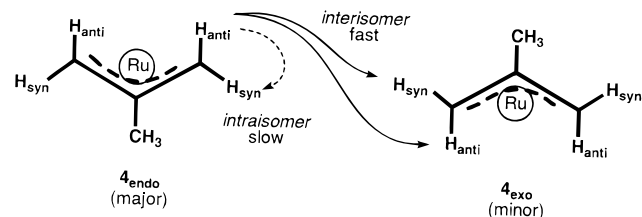

Figure 9. Schematic representation of the relative rates of exchange of allyl proton sites in complex **4**.

Figure 10. Evolution of magnetization transfer over time. Data are normalized peak volumes taken from EXSY spectra at 10, 20, 40, and 100 ms and correspond to magnetization transfer from the *anti* site of **4$_{exo}$** (the minor isomer) to all other allyl sites: (■) **4$_{exo}$** (minor) *anti* site; (●) **4$_{exo}$** (minor) *syn* site; (◇) **4$_{endo}$** (major) *anti* site; (◆) **4$_{endo}$** (major) *syn* site; (□) **4$_{endo}$** (major) sum of *anti* and *syn* sites.

be calculated: $k_{min \rightarrow maj} = 17.8 \pm 2.4$ s^{-1} ($\Delta G^{\ddagger} = 17.4 \pm 0.1$ kcal mol^{-1}) and $k_{maj \rightarrow min} = 2.9 \pm 0.2$ s^{-1} ($\Delta G^{\ddagger} = 18.6 \pm 0.1$ kcal mol^{-1}). Quantitative analysis of the exchange rates was also performed with the D2DNMR program developed by Orrell and coworkers and shows excellent agreement.[39] This method determines the rates of multisite exchange from the EXSY spectrum crosspeak volumes. The calculated first-order rate

(39) Abel, E. W.; Coston, T. P. J.; Orrell, K. G.; Sik, V.; Stephenson, D. *J. Mag. Reson.* **1986**, *70*, 34.
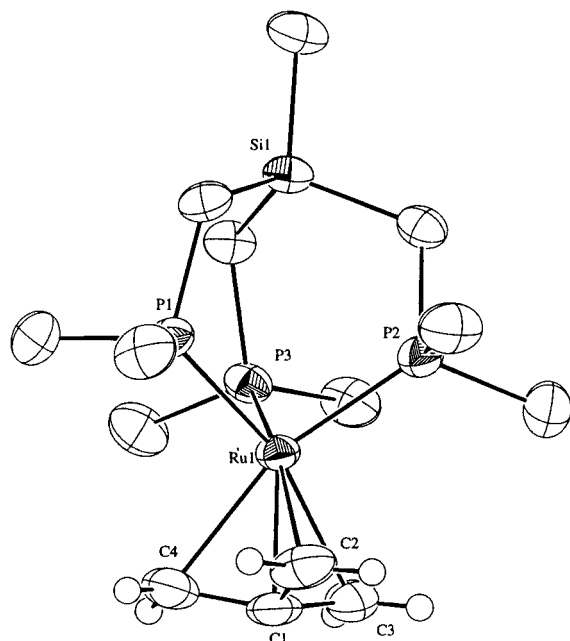
Figure 11. ORTEP diagram of **7**. See Table 3 for selected metrical parameters.

constants at 54.9 °C are $k_{min \to maj} = 19.9 \pm 2.4$ s^{-1} ($\Delta G^{\ddagger} = 17.3 \pm 0.1$ kcal mol^{-1}) and $k_{maj \to min} = 2.4 \pm 0.2$ s^{-1} ($\Delta G^{\ddagger} = 18.7 \pm 0.1$ kcal mol^{-1}), corresponding to $\Delta G_{maj \to min}$(328 K) = 1.4 ± 0.1 kcal mol^{-1}.

Preparation of SiP$_3$Ru(η^4-C(CH$_2$)$_3$) (7) by Thermolysis of 4. Heating isolated samples of **4** in toluene solution (135 °C, 3 days) resulted in the formation of SiP$_3$Ru(TMM) (TMM = η^4-C(CH$_2$)$_3$), **7** (eq 6). When the reaction was monitored by
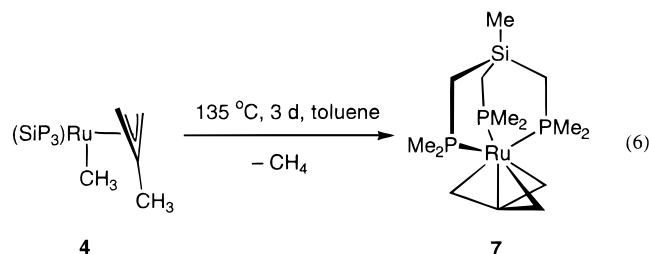

^{1}H NMR spectroscopy, clean formation of **7** and CH$_4$ was observed. The solid-state structure of **7** was determined by a single-crystal X-ray diffraction experiment. An ORTEP diagram of **7** is shown in Figure 11. The TMM ligand is found to be folded toward the Ru center with the plane formed by C2, C3, and C4 being 0.31 Å above C1, the central carbon atom. The umbrella-like puckering of the TMM ligand has been quantified in terms of the angle θ.[40] Complex **7** has $\theta = 12.5°$, which matches that seen in most other TMM complexes ($\theta \approx 12°$).[40] A comparison of some metrical parameters of **7** with those of (CO)$_3$Ru(TMM) and (η^6-C$_6$H$_6$)Ru(TMM) is given in Table 2.

The reversibility of formation of **7** from **4** was probed by heating **7** in the presence of CD$_4$. At temperatures up to 175 °C, no deuterium incorporation into **7** was observed, indicating the reaction is irreversible under these conditions.

Discussion

The overall process observed in this work is the stepwise degradation of a neopentyl (C$_5$H$_{11}$$^-$) ligand to a trimethylene-methane (C$_4$H$_6$$^{2-}$) ligand in three discrete steps (eq 7): cyclo-

metalation/elimination, β-methyl transfer, and then a second cyclometalation/elimination. The central step is a rare example of reversible C−C activation.
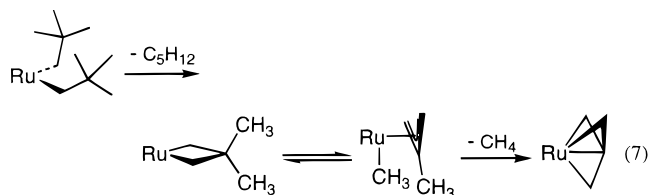
Examples of 2,2-dimethylmetallacyclobutanes have been reported for a large variety of metals.[41−63] Synthesis of metallacycles of this type via cyclometalation of a neopentyl ligand has been found to be relatively general for the late transition metals.[41] Comprehensive mechanistic studies on the cyclometalation of a neopentyl ligand[59,61,63] have led us to propose the mechanism in Scheme 2. Consistent with this proposed mechanism is the observation of **1**-d_2 from **3** and Me$_3$-CCD$_2$MgBr (Scheme 1).

Considering the second step of this process in more detail, metallacyclobutanes have been described as having three basic routes to rearrangement and decomposition: retrocyclization, β-elimination, and reductive elimination (Scheme 3).[43,64] When the β-carbon is substituted, as in **1**, the β-elimination process is usually blocked, leaving [2 + 2] retrocyclization and reductive elimination of cyclopropanes as the dominant decomposition

(40) Jones, M. D. *Adv. Organomet. Chem* **1987**, *27*, 279.

(41) Jennings, P. W.; Johnson, L. L. *Chem. Rev.* **1994**, *94*, 2241.

(42) Bickelhaupt, F. *J. Organomet. Chem.* **1994**, *475*, 1.

(43) Grubbs, R. H. In *Comprehensive Organometallic Chemistry*; Wilkinson, G., Ed.; Pergamon: Oxford, England, 1982; Vol. 8, p 499.

(44) Feldman, J.; Schrock, R. R. *Prog. Inorg. Chem.* **1991**, *39*, 1.

(45) Ti: Lee, J. B.; Gajda, G. J.; Schaefer, W. P.; Howard, T. R.; Ikariya, T.; Straus, D. A.; Grubbs, R. H. *J. Am. Chem. Soc.* **1981**, *103*, 7358.

(46) Ti: Straus, D. A.; Grubbs, R. H. *Organometallics* **1982**, *1*, 1658.

(47) Zr, Hf: Seetz, J. W. F. L.; Schat, G.; Akkerman, O. S.; Bickelhaupt, F. *Angew. Chem., Int. Ed. Engl.* **1983**, *22*, 248.

(48) V: Seetz, J. W. F. L.; Heisteeg, B. J. J. v. d.; Schat, G.; Akkerman, O. S.; Bickelhaupt, F. *J. Organomet. Chem.* **1984**, *275*, 173.

(49) Mo, W: Boer, H. J. R. d.; Heisteeg, B. J. J. v. d.; Schat, G.; Akkerman, O. S.; Bickelhaupt, F. *J. Organomet. Chem.* **1988**, *346*, 197.

(50) Re: Boer, H. J. R. d.; Heisteeg, B. J. J. v. d.; Flöel, M.; Herrmann, W. A.; Akkerman, O. S.; Bickelhaupt, F. *Angew. Chem., Int. Ed. Engl.* **1987**, *26*, 73.

(51) Ru: Andersen, R. A.; Jones, R. A.; Wilkinson, G. *J. Chem. Soc., Dalton Trans.* **1979**, 446. The ruthenacyclobutane, (PMe$_3$)$_4$Ru(CH$_2$CMe$_2$-CH$_2$), also undergoes the β-methyl elimination reaction giving (PMe$_3$)$_3$-Ru(η^3-CH$_2$CMeCH$_2$) when heated in C$_6$D$_6$ to 75 °C for 12 h: McNeill, K.; Andersen, R. A.; Bergman, R. G. Unpublished results.

(52) Ru: Diversi, P.; Ingrosso, G.; Lucherini, A.; Marchetti, F.; Adovasio, V.; Nardelli, M. *J. Chem. Soc., Dalton Trans.* **1991**, 203.

(53) Ru: Adovasio, V.; Diversi, P.; Ingrosso, G.; Lucherini, A.; Marchetti, F.; Nardelli, M. *J. Chem. Soc., Dalton Trans.* **1992**, 3385.

(54) Os: Bennett, M. A.; Weerasuria, A. M. M. *J. Organomet. Chem.* **1990**, *394*, 481.

(55) Rh: Diversi, P.; Ingrosso, G.; Lucherini, A.; Fasce, D. *J. Chem. Soc., Chem. Commun.* **1982**, 945.

(56) Rh: Andreucci, L.; Diversi, P.; Ingrosso, G.; Lucherini, A.; Marchetti, F.; Adovasio, V.; Nardelli, M. *J. Chem. Soc., Dalton Trans.* **1986**, 477.

(57) Ir: Tulip, T. H.; Thorn, D. L. *J. Am. Chem. Soc.* **1981**, *103*, 2448.

(58) Ir: Andreucci, L.; Diversi, P.; Ingrosso, G.; Lucherini, A.; Marchetti, F.; Adovasio, V.; Nardelli, M. *J. Chem. Soc., Dalton Trans.* **1986**, 803.

(59) Ir: Harper, T. G. P.; Desrosiers, P. J.; Flood, T. C. *Organometallics* **1990**, *9*, 2523.

(60) Ni, Pd: Miyashita, A.; Ohyoshi, M.; Shitara, H.; Nohira, H. *J. Organomet. Chem.* **1988**, *338*, 103.

(61) Pt: Foley, P.; DiCosimo, R.; Whitesides, G. M. *J. Am. Chem. Soc.* **1980**, *102*, 6713.

(62) Pt: Cushman, B. M.; Brown, D. B. *Inorg. Chem.* **1981**, *20*, 2490.

(63) Th: Bruno, J. W.; Marks, T. J.; Day, V. W. *J. Am. Chem. Soc.* **1982**, *104*, 7357.

(64) Koppen, P. A. M. v.; Jacobson, D. B.; Illies, A.; Bowers, M. T.; Hanratty, M.; Beauchamp, J. L. *J. Am. Chem. Soc.* **1989**, *111*, 1991.

Table 2. Comparison of Structural Features in Ru(TMM) Complexes

complex	Ru−$C_{central}$ (Å)	Ru−C_{tmm} (av) (Å)	C−C_{tmm} (av) (Å)	pyramid angle (θ)	ref
(SiP₃)Ru(TMM)	2.062(3)	2.239(4)	1.431(7)	12.4	this work
(CO)₃Ru(TMM)	2.055(5)	2.255(5)	1.410(28)	12.0	103
(η^6-C₆H₆)Ru(TMM)	2.029(3)	2.186(12)	1.429(13)	13.8	102, 103

Scheme 2
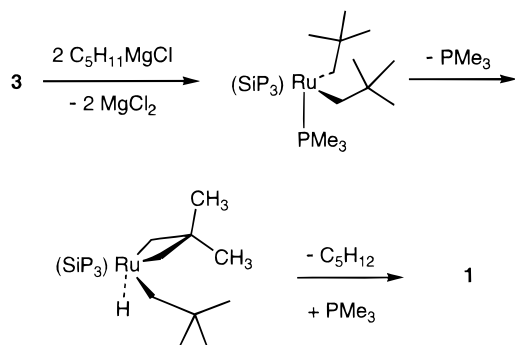
Scheme 3
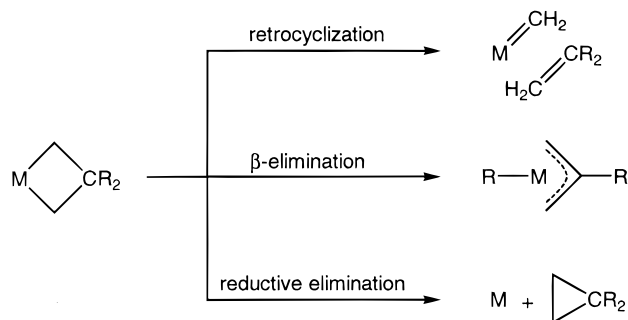
Scheme 4
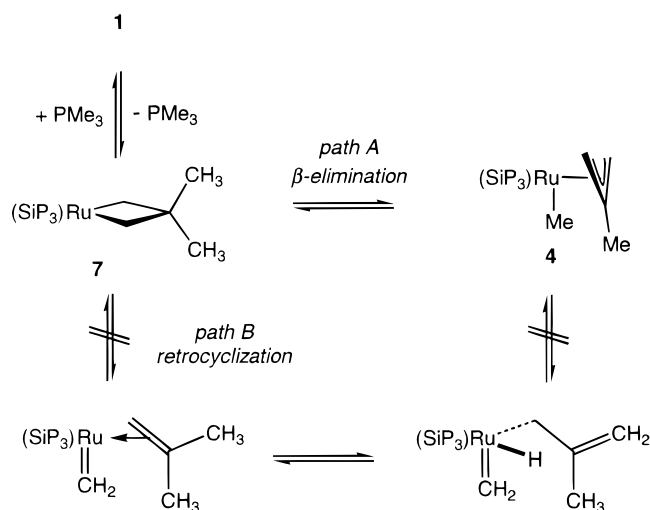
pathways. It was therefore surprising that the product obtained from heating **1** was the apparent product of β-elimination. Upon further consideration, it was possible to conceive of a mechanism for this step that proceeded through the retrocyclization pathway. The alternate pathway, path B, proceeds via retrocyclization, allylic C−H activation, and α-H migration (Scheme 4). Because retrocyclization is the more common C−C cleavage process for metallacyclobutanes, this more complicated process had to be considered.
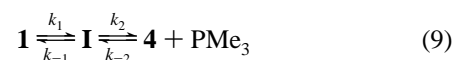
The results of the thermolysis of **1-d_2**, discussed above, provide a way of distinguishing between paths A and B. Path B predicts scrambling of the deuterium label into the methyl

site of **4**, whereas path A requires retention of the label in the methylene sites of **4**. Thermolysis of **1-d_2** yields **4** labeled exclusively in the methylene sites. The lack of label scrambling into the methyl site excludes the retrocyclization path (B) and provides support for the β-methyl elimination path (A).

Kinetic Studies. For the interconversion of **1** and **4**, kinetics for the approach to equilibrium from **1** were observed (eq 8).
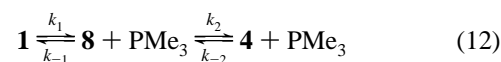
$$\mathbf{1} \rightleftharpoons \mathbf{4} + PMe_3 \tag{8}$$

In these studies, [PMe₃] was kept in excess to simplify the kinetic behavior of the system. The fact that the equilibrium is composed of opposing reactions that are both first order and second order results in two possible predictions for the effect of [PMe₃] on the observed rate constant. If PMe₃ is lost after (or during) the rate-controlling step in the forward direction (eq 9), then the system is kinetically indistinguishable from a direct transformation (eq 10). In this case, [PMe₃] will not affect the

$$\mathbf{1} \underset{k_{-1}}{\overset{k_1}{\rightleftharpoons}} \mathbf{I} \underset{k_{-2}}{\overset{k_2}{\rightleftharpoons}} \mathbf{4} + PMe_3 \tag{9}$$

$$\mathbf{1} \underset{k_r}{\overset{k_f}{\rightleftharpoons}} \mathbf{4} + PMe_3 \tag{10}$$

forward rate and will increase the back rate. The observed rate constant, k_{obs}, should vary linearly with [PMe₃] (eq 11).[38]

$$k_{obs} = k_f + k_r[PMe_3] \tag{11}$$

If PMe₃ is lost *prior* to the rate-controlling transition state in the forward direction (eq 12), then the forward rate is depressed by added PMe₃ and the back rate is unaffected. In this case, k_{obs} will have a more complicated dependence (eq 13). At high

$$\mathbf{1} \underset{k_{-1}}{\overset{k_1}{\rightleftharpoons}} \mathbf{8} + PMe_3 \underset{k_{-2}}{\overset{k_2}{\rightleftharpoons}} \mathbf{4} + PMe_3 \tag{12}$$

$$k_{obs} = \frac{k_1 k_2}{k_{-1}[PMe_3] + k_2} + \frac{k_{-1}k_{-2}[PMe_3]}{k_{-1}[PMe_3] + k_2} \tag{13}$$

[PMe₃], if $k_{-1}[PMe_3] \gg k_2$, eq 13 is simplified and k_{obs} will vary inversely with [PMe₃] (eq 14). In this way it is possible to distinguish between mechanisms that require PMe₃ dissociation prior to the rate-controlling step and those that do not.

$$k_{obs} = \frac{k_1 k_2}{k_{-1}[PMe_3]} + k_{-2} \qquad (k_{-1}[PMe_3] \gg k_{-2}) \tag{14}$$

The kinetic data presented in this work are consistent with a two-step process that involves reversible dissociation of PMe₃ from **1** followed by a reversible unimolecular rearrangement to give **4**. Because the observed rate for the approach to equilibrium varies inversely with [PMe₃] (Figure 5), it is clear that the PMe₃-dissociation step precedes the rate-controlling step in the forward direction. This indicates that the reaction does not involve loss of an arm of the tridentate SiP₃ ligand and suggests that the SiP₃ ligand is kinetically less labile than the monodentate PMe₃ ligand.

The microscopic rate constants, k_2 and k_{-2}, correspond to the rates for β-elimination and β-insertion, respectively. It is not possible to obtain a value for k_2 from these studies, but k_{-2} can be obtained by combining the expression for K_{eq}, eq 15, with eq 14 (eq 16).
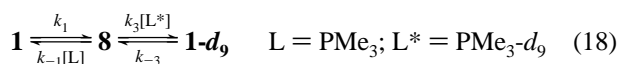
$$K_{eq} = \frac{k_1 k_2}{k_{-1} k_{-2}} = \frac{[\mathbf{4}][PMe_3]}{[\mathbf{1}]} \qquad (15)$$

$$k_{-2} = \frac{k_{obs}}{\dfrac{K_{eq}}{[PMe_3]} + 1} \qquad (16)$$

The temperature dependence of k_{-2} was measured (73.6–117.3 °C) and provided activation parameters for the β-methyl insertion step: $\Delta G^{\ddagger}_{363.7} = 28.6 \pm 0.7$ kcal mol^{-1}, $\Delta H^{\ddagger} = 26.0 \pm 1.2$ kcal mol^{-1}, and $\Delta S^{\ddagger} = -10.5 \pm 0.9$ cal K^{-1} mol^{-1}. The relatively small, negative value for the entropy of activation is consistent with a unimolecular process in which the transition state is more ordered than the ground state (eq 17). This value is similar to those found for β-H and β-alkyl migratory insertion.[65–68]

$$(17)$$
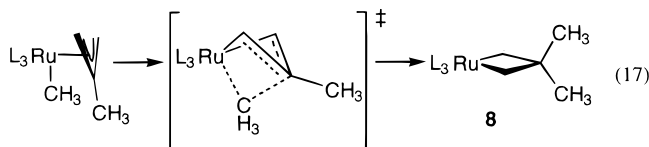
A value for k_1, the rate constant for PMe$_3$ dissociation, was obtained by measuring the rate of exchange with PMe$_3$-d_9. The kinetic analysis for a dissociative ligand substitution process (eq 18) is similar to that described above as it is two consecutive

$$\mathbf{1} \underset{k_{-1}[L]}{\overset{k_1}{\rightleftharpoons}} \mathbf{8} \underset{k_{-3}}{\overset{k_3[L^*]}{\rightleftharpoons}} \mathbf{1}\text{-}d_9 \qquad L = PMe_3; \; L^* = PMe_3\text{-}d_9 \quad (18)$$

equilibria. The calculated expression for k_{obs} is again composed of two terms that correspond to the forward and reverse rate constants (eqs 19 and 20). Flooding with PMe$_3$-d_9, such that

$$k_{obs} = \frac{k_1 k_3[L^*]}{k_{-1}[L] + k_3[L^*]} + \frac{k_{-1} k_{-3}[L]}{k_{-1}[L] + k_3[L^*]} \qquad (19)$$

$$K_{eq} = \frac{k_1 k_3}{k_{-1} k_{-3}} = \frac{[\mathbf{1}\text{-}d_9][L]}{[\mathbf{1}][L^*]} \qquad (20)$$

$k_3[PMe_3\text{-}d_9] \gg k_{-1}[PMe_3]$, simplifies the expression for k_{obs} (eq 21).

$$k_{obs} = k_1 + \frac{k_{-1} k_{-3}[L]}{k_3[L^*]} \qquad (k_3[L^*] \gg k_{-1}[L]) \quad (21)$$

Combination of the expressions in eqs 20 and 21 gives an expression for k_1 in terms of k_{obs} and K_{eq}, both measurable quantities (eq 22). An exchange reaction was performed at -10.2 °C, and the calculated value for k_1 was determined to be $(8.36 \pm 0.15) \times 10^{-5}$, corresponding to $\Delta G^{\ddagger}_{263.0} = 20.24 \pm 0.01$ kcal mol^{-1}.

$$k_1 = \frac{k_{obs}}{\dfrac{[L^*]}{K_{eq}[L]} + 1} \qquad (22)$$

From the kinetic and equilibrium studies, a nearly complete picture of the β-methyl elimination/insertion develops (Figure 13). The data support a two-step, reversible process in which PMe$_3$ is lost in the fast, first step, opening a coordination site, and the methyl group is transferred from the hydrocarbyl ligand to the metal in the slow, second step. The overall reaction is *endothermic*; the reaction is driven entropically by the loss of PMe$_3$. Marks *et al.* have calculated the enthalpies of reaction for a series of β-alkyl elimination reactions at the Cp*$_2$Zr fragment based on their extensive thermochemical studies. They predict that the processes will vary between endothermic ($+20$ kcal mol^{-1}) and weakly exothermic (-6 kcal mol^{-1}) depending on the substrate.[69]

The reversible C–C cleavage demonstrated here lends strong support to the previously proposed β-methyl and β-phenyl transfer reactions in the chemistry of ruthenium oxametallacyclobutanes (Scheme 5).[30] Furthermore, the η^3-oxallyl intermediate proposed earlier on the basis of kinetic evidence is supported by the observation of its all-carbon analog in this work.

The reversibility of methyl transfer between the ruthenium center and the π-allyl ligand is similar in many regards to that seen by Green,[70] Eilbracht,[71–75] Crabtree,[76,77] and most recently Wolczanski.[78] In 1974, Benfield and Green reported the reversible transfer of an ethyl group between the Cp ligand and the metal in Cp$_2$MoEtCl.[70] Wolczanski has extended this class of reactions to arene ligands bound to ruthenium.[78]

Dynamic Interchange of the Isomers of 4. The EXSY data for the interconversion of $\mathbf{4}_{endo}$ and $\mathbf{4}_{exo}$ (see eq 2) are interesting in that they require a very specific mechanism for the process. It is clear from the data that an η^3-η^1-η^3 mechanism, as seen in other systems,[79,80] is operative. In such a mechanism, rotation about the C–C single bond in the η^1-allyl species interconverts the isomers. If one were to label just the *syn* protons of the major isomer, the boxed hydrogens in eq 23, this mechanism requires that the label be split between the *syn* and *anti* sites of the minor isomer upon major–minor interconversion (eq 23).

$$(23)$$

major   minor

The EXSY data agree with these predictions. A more subtle

(65) Roe, D. C. *J. Am. Chem. Soc.* **1983**, *105*, 7770.
(66) Doherty, N. M.; Bercaw, J. E. *J. Am. Chem. Soc.* **1985**, *107*, 2670.
(67) Wang, L.; Flood, T. C. *J. Am. Chem. Soc.* **1992**, *114*, 3169.
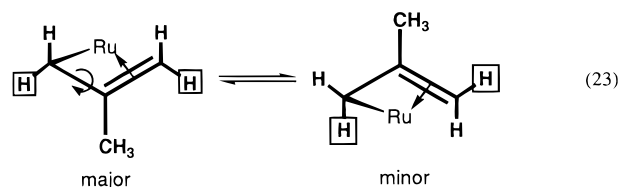(68) Rix, F. C.; Brookhart, M.; White, P. S. *J. Am. Chem. Soc.* **1996**, *118*, 2436.
(69) Schock, L. E.; Marks, T. J. *J. Am. Chem. Soc.* **1988**, *110*, 7701.
(70) Benfield, F. W. S.; Green, M. L. H. *J. Chem. Soc., Dalton Trans.* **1974**, 1324.
(71) Eilbracht, P. *Chem. Ber.* **1976**, *109*, 1429.
(72) Eilbracht, P.; Dahler, P. *Chem. Ber.* **1980**, *113*, 542.
(73) Eilbracht, P.; Dahler, P.; Mayser, U.; Henkes, E. *Chem. Ber.* **1980**, *113*, 1033.
(74) Eilbracht, P.; Mayser, U.; Tiedtke, G. *Chem. Ber.* **1980**, *113*, 1420.
(75) Eilbracht, P.; Mayser, U. *Chem. Ber.* **1980**, *113*, 2211.
(76) Crabtree, R. H.; Dion, R. P. *J. Chem. Soc., Chem. Commun.* **1984**, 1260.
(77) Crabtree, R. H.; Dion, R. P.; Gibboni, D. J.; McGrath, D. V.; Holt, E. M. *J. Am. Chem. Soc.* **1986**, *108*, 7222.
(78) DiMauro, P. T.; Wolczanski, P. *Polyhedron* **1995**, *14*, 149.
(79) Faller, J. W. *Adv. Organomet. Chem.* **1977**, *16*, 211.
(80) Mann, B. E. In *Comprehensive Organometallic Chemistry*; Wilkinson, G., Stone, F. G. A., Abel, E. W., Eds.; Pergamon: London, 1982; Vol. 3, p 110.
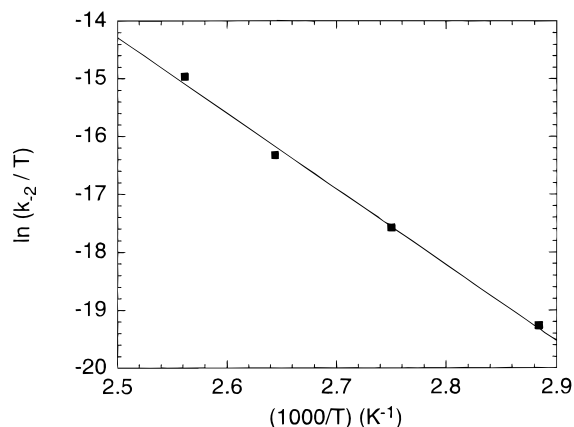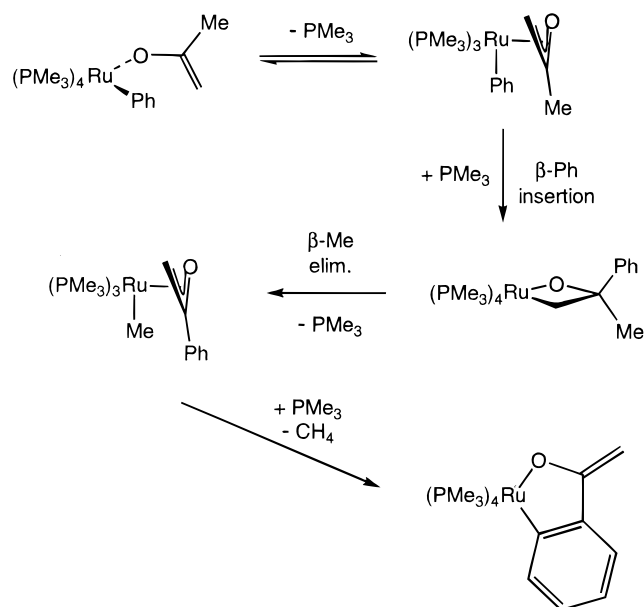
Figure 12. Temperature dependence of k_{-2} (73.6 < T < 117.3 °C).

Scheme 5

point is that exchange of the *syn* and *anti* sites is possible without major/minor isomerization. Such *intra*isomer exchange would occur if the η^1-allyl intermediate contains a mirror plane by having trigonal bipyramidal geometry or a time-averaged mirror plane by rapid interconversion of the two enantiomeric square pyramid forms (eq 24).
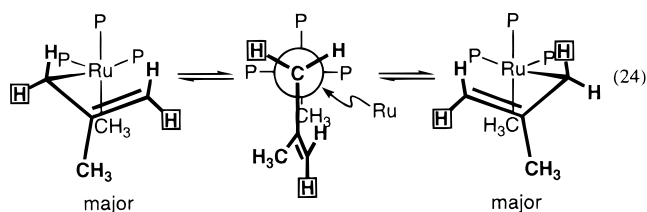
In **4**, it is observed that no *intra*isomer scrambling of the magnetic label occurs during the experiment, requiring that the η^1-allyl intermediate does not have a real or time-averaged mirror plane of symmetry. In other words, on the time scale of the major−minor interconversion, the η^1-intermediate species is stereochemically rigid and does not have a trigonal bipyramidal coordination geometry.

From consideration of orbital symmetry, this seems reasonable. For a d^6 transition metal, one would expect a square-pyramidal ground state for the five-coordinate η^1-allyl species and a barrier to interconversion with its enantiomer (proceeding
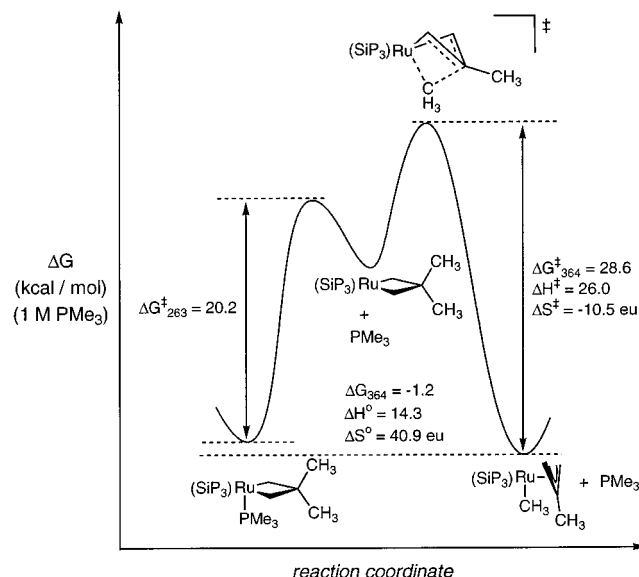

Figure 13. Reaction coordinate diagram for the interconversion of **1** and **4**.

through a mirror symmetric transition state).[81,82] In general, solid state structures of 5-coordinate ruthenium(II) complexes display square pyramid geometry.[83−95] Hoffman and Caulton have reported activation enthalpies for square pyramid inter-conversion in (PPh$_3$)$_3$RuCl$_2$ and (PPh$_3$)$_3$RuHCl to be 10.0 and 13.4 kcal mol^{-1}, respectively.[96,97] It has also been shown that the effect of a chelating phosphine on the barrier is minor.[98]

In summary, the EXSY data provide an unusually detailed picture of the stereochemical behavior of the metal complex outlining both the mechanism of exchange and the structure of the intermediate species (Figure 14). In converting an η^3-allyl

(81) Albright, T. A.; Burdett, J. K.; Whangbo, M.-H. *Orbital Interactions in Chemistry*; John Wiley & Sons, Inc.: New York, 1985.

(82) Riehl, J.-F.; Jean, Y.; Eisenstein, O.; Pélissier, M. *Organometallics* **1992**, *11*, 729.

(83) LaPlaca, S. J.; Ibers, J. A. *Inorg. Chem.* **1965**, *4*, 778. The authors report the structure of (PPh$_3$)$_3$RuCl$_2$ in which there appears to be an agostic interaction with one of the phenyl C−H bonds and the metal center. The Os analog was found to be free of any agostic interactions: Chakravarty, A. R.; Cotton, F. A.; Tocher, D. A. *Acta Crystallogr.* **1985**, *C41*, 698.

(84) Cotton, F. A.; Matusz, M. *Inorg. Chim. Acta* **1987**, *131*, 213.

(85) Albinati, A.; Jiang, Q.; Rüegger, H.; Venanzi, L. M. *Inorg. Chem.* **1993**, *32*, 4940.

(86) Rickard, C. E. F.; Roper, W. R.; Taylor, G. E.; Waters, J. M.; Wright, L. J. *J. Organomet. Chem.* **1990**, *389*, 375.

(87) Torres, M. R.; Vegas, A.; Santos, A.; Ros, J. *J. Organomet. Chem.* **1986**, *309*, 169.

(88) Owen, M. A.; Pye, P. L.; Piggott, B.; Capparelli, M. B. *J. Organomet. Chem.* **1992**, *434*, 351.

(89) Huang, D.; Heyn, R. H.; Bollinger, J. C.; Caulton, K. G. *Organometallics* **1997**, *16*, 292.

(90) Mudalige, D. C.; Retting, S. J.; James, B. R.; Cullen, W. R. *J. Chem. Soc., Chem. Commun.* **1993**, 830.

(91) Pedersen, A.; Tilset, M.; Folting, K.; Caulton, K. G. *Organometallics* **1995**, *14*, 875.

(92) The following two references have structures described as distorted trigonal bipyramids: Skapski, A. C.; Troughton, P. G. H. *J. Chem. Soc., Chem. Commun.* **1968**, 1230.

(93) Mezzetti, A.; Zotto, A. D.; Rigo, P.; Pahor, N. B. *J. Chem. Soc., Dalton Trans.* **1989**, 1045.

(94) Wakatsuki, Y.; Yamazaki, H.; Maruyama, Y.; Shimizu, I. *J. Organomet. Chem.* **1992**, *430*, C60. Described here are compounds which are "half-way" between 5- and 6-coordinate due to allyl ligands which are "half-way" between η^1- and η^3-bound.
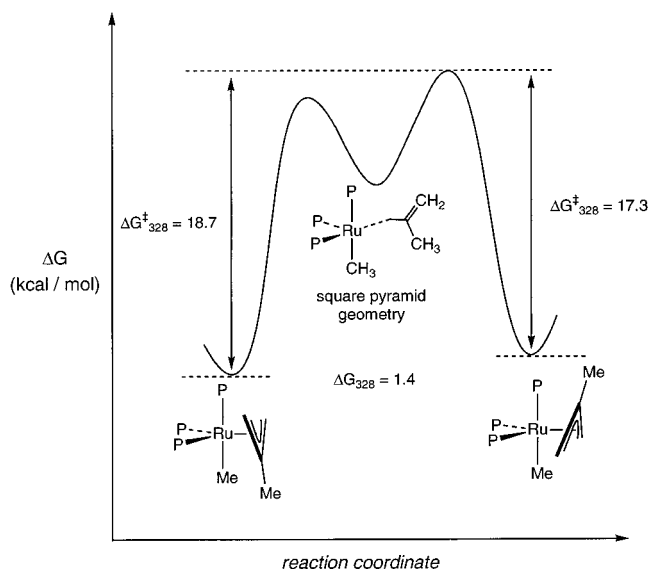
(95) MacFarlane, K. S.; Joshi, A. M.; Rettig, S. J.; James, B. R. *Inorg. Chem.* **1996**, *35*, 7304.

(96) Hoffman, P. R.; Caulton, K. G. *J. Am. Chem. Soc.* **1975**, *97*, 4221.

(97) It should be noted that while there is no need to postulate an agostic interaction, 5-coordinate Ru(II) complexes often display such interactions.

(98) Jung, C. W.; Garrou, P. E.; Hoffman, P. R.; Caulton, K. G. *Inorg. Chem.* **1984**, *23*, 726.

Figure 14. Reaction coordinate diagram for the interconversion of **4$_{endo}$** and **4$_{exo}$**.

complex to its isomer, a pseudo-square pyramid intermediate is formed. Presumably this intermediate can interconvert with its enantiomer. However, this process is slow compared with the η^3-η^1-η^3 process. The result is that experimentally one observes no *intra*isomer exchange of magnetization at early mixing times. Only after hundreds of milliseconds—after there have been many interconversion events—does one see the magnetization of a given allyl site become distributed among all of the allyl positions.

Trimethylenemethane Complex. The formation of complex **7** is the only example, to our knowledge, of a reaction in which a trimethylenemethane (TMM) ligand is derived from a neopentyl ligand.[40,99] The final step in the three-step degradation of the neopentyl group, loss of methane from a complex containing a methyl and methallyl ligand, has been observed previously.[100,101] Herberich and co-workers have reported two close analogs of **7**, $(CO)_3Ru(TMM)$ and $(\eta^6\text{-}C_6H_6)Ru\text{-}$(TMM).[102,103] The Ru(TMM) fragment in complex **7** is more similar structurally to the carbonyl complex, showing an analogous strong *trans* influence.

Conclusion

In summary, a thorough understanding of the degradation of a neopentyl ligand to a trimethylenemethane ligand has been achieved. Throughout this investigation, the SiP$_3$ ligand has played a crucial role. The complexes studied with this tripodal ligand have been shown to have a kinetically stable and structurally well-defined (SiP$_3$)Ru fragment. The NMR properties of the ligand have allowed unambiguous assignment of structure of isolable species and reactive intermediates. In contrast to the analogous systems containing all monodentate or polydentate phosphine ligands, kinetic studies with the (SiP$_3$)(PMe$_3$)Ru system identify both the occurrence of ligand dissociation and the location of the open coordination site.

Experimental Section

General Methods. All reactions were performed under inert atmosphere (N$_2$ or Ar). A description of instrumentation and general procedures has been published.[104] Unless otherwise specified, all reagents were purchased from commercial suppliers and used without further purification. PMe$_3$ (Strem or Aldrich) was dried over Na prior to use. Neopentyl chloride (Aldrich) and 3-bromo-2-methylpropene (Aldrich) were dried over P$_2$O$_5$ prior to use. Me$_3$CCD$_2$MgBr was prepared according to literature procedures.[105,106] (SiP$_3$)(PMe$_3$)RuCl$_2$ (**3**) was prepared by the method of Dahlenburg.[107]

NMR Spectroscopy. Two-dimensional NMR experiments were performed on a Bruker AMX spectrometer (^{1}H, 300.13 MHz; ^{13}C, 75.33 MHz; ^{31}P, 121.55 MHz) equipped with an inverse probe. The EXSY data were acquired at 54.9 °C, the temperature being calibrated against an ethylene glycol chemical shift standard. The NOESY and EXSY experiments were performed with the Bruker pulse program, noesytp, modified by Dr. Graham Ball such that the data were ^{31}P decoupled. Rate constants for the exchange data were calculated by the method of Orrel *et al.*[39] and as described above.

Kinetic and Equilibrium Measurements. For the kinetic studies of the conversion of **1** to **4**, solutions containing **1** (20 mM), *p*-(MeO)$_2$C$_6$H$_4$ (5.4 mM), and PMe$_3$ (0.25–1.9 M) in toluene-d_8 were employed. The samples either were placed in constant temperature baths (73.6 to 117.3 °C) where the reaction progress was monitored by ^{1}H{^{31}P} NMR at 25 °C or the reaction was followed in the NMR probe with the temperature calibrated by an ethylene glycol standard. The reactions were usually followed to >3 half-lives. The calculated infinity points from these runs provided the equilibrium concentrations of **1**, **4**, and PMe$_3$. The PMe$_3$/PMe$_3$-d_9 exchange reactions were performed with **1** (12 mM), *p*-(MeO)$_2$C$_6$H$_4$ (4.4 mM), and PMe$_3$-d_9 (0.25 M), and were followed in the probe at 263 K. Commercial software was used to fit data and calculate end points.[108]

***trans*-(PMe$_3$)$_4$RuCl$_2$.** The following synthesis was found to be more convenient than the published procedure.[109,110] A 500-mL, three-necked round-bottom flask equipped with a stir bar and condenser was charged with RuCl$_3$·xH$_2$O (8.5 g, 35 mmol), PMe$_3$ (25 g, 330 mmol, 9.4 equiv), and degassed MeOH (300 mL). The solution was heated at reflux for 5 h. Upon cooling, orange crystals precipitated from solution. The mother liquor was removed by cannula. The precipitate was washed with cold, degassed MeOH (4 × 10 mL) and dried *in vacuo* (11.84 g, 71% yield). ^{1}H NMR (400 MHz, C$_6$D$_6$): δ 1.35 (vt, J = 2.4 Hz). ^{31}P{^{1}H} NMR (162 MHz, C$_6$D$_6$): δ −5.64 (s). Lit.[109] ^{1}H NMR (C$_6$D$_6$): δ 1.40. ^{31}P{^{1}H} NMR (C$_6$D$_6$): δ −6.95 (s).

MeSi(CH$_2$PMe$_2$)$_3$ (SiP$_3$). The following synthesis was found to be more convenient than the published procedure.[111] A 2-L two-necked flask equipped with an addition funnel (200 mL) and a magnetic stir bar was charged with LiCH$_2$PMe$_2$[112] (11.9 g , 180 mmol; CAUTION: highly pyrophoric solid) and 1.0 L of Et$_2$O. MeSiCl$_3$ (8.6 g, 57 mmol) was diluted with 120 mL of Et$_2$O and added to the addition funnel by cannula. The reaction flask was cooled to −78 °C and the chlorosilane added with vigorous stirring over 2.5 h. Following addition, the reaction mixture was allowed to warm to 25 °C, and the volatile materials were removed *in vacuo*. The resultant brownish oil was extracted with pentane (4 × 50 mL). The pentane extracts were flushed through a short column of silica gel (2.5 cm diameter × 2.5 cm). The column was subsequently washed with pentane (2 × 10 mL) and Et$_2$O (2 × 10 mL). The combined column fractions were exposed to dynamic vacuum overnight. The oil was distilled under active vacuum (ca. 0.01 Torr, 75 °C) with use of a short path still to yield a colorless liquid (7.7 g, 30 mmol, 52% yield). ^{1}H NMR (400 MHz, C$_6$D$_6$): δ 0.95 (18

(99) Marr, G.; Rockett, B. W. In *The Chemistry of the Metal–Carbon Bond*; Hartley, F. R., Patai, S., Eds.; John Wiley & Sons: New York, 1982; p 367.

(100) Mayer, J. M.; Curtis, C. J.; Bercaw, J. E. *J. Am. Chem. Soc.* **1983**, *105*, 2651.

(101) Rodriguez, G.; Bazan, G. C. *J. Am. Chem. Soc.* **1997**, *119*, 343.

(102) Herberich, G. E.; Spaniol, T. P. *J. Chem. Soc., Chem. Commun.* **1991**, 1457.

(103) Herberich, G. E.; Spaniol, T. P. *J. Chem. Soc., Dalton Trans.* **1993**, 2471.

(104) Meyer, K. E.; Walsh, P. J.; Bergman, R. G. *J. Am. Chem. Soc.* **1995**, *117*, 974.

(105) Caulton, K. G.; Chisholm, M. H.; Streib, W. E.; Xue, Z. *J. Am. Chem. Soc.* **1991**, *113*, 6082.

(106) Legdzins, P.; Retting, S. J.; Veltheer, J. E.; Batchelor, R. J.; Einstein, F. W. B. *Organometallics* **1993**, *12*, 3375.

(107) Dahlenburg, L.; Kerstan, S.; Werner, D. *J. Organomet. Chem.* **1991**, *411*, 457.

(108) *KaleidaGraph*; 3.06 ed.; Synergy Software, 1986–1996.

(109) Schmidbaur, H.; Blaschke, G. *Z. Naturforsch. B* **1980**, *356*, 584.

(110) Sellman, D.; Bohlen, E. *Z. Naturforsch. B* **1982**, *37*, 1026.

(111) Karsch, H. H.; Appelt, A. *Z. Naturforsch. B* **1983**, *38*, 1399.

(112) Karsch, H. H.; Schmidbaur, H. *Z. Naturforsch. B* **1977**, *32*, 762.

H, d, J = 6.7 Hz), 0.73 (6 H, d, J = 1.4 Hz), 0.29 (3 H, s). ^{31}P{^{1}H} NMR (162 MHz, C$_6$D$_6$): δ −55.0 (s, $^{2}J_{P-{}^{29}Si}$ = 7.2 Hz). Lit.[111] ^{1}H NMR (C$_6$D$_6$): δ 1.00 (18 H, d, J = 3 Hz), 0.75 (6 H, d, J = 1.4 Hz), 0.25 (3 H, q, J = 0.8 Hz). ^{31}P{^{1}H} NMR (162 MHz, C$_6$D$_6$): δ −56.4.

(SiP$_3$)(PMe$_3$)Ru(CH$_2$CMe$_2$CH$_2$) (1). To a solution of (SiP$_3$)(PMe$_3$)-RuCl$_2$ (3) (365 mg, 0.71 mmol) in THF (50 mL) in a 100-mL glass bomb was added a Et$_2$O solution of Me$_3$CCH$_2$MgCl (0.66 M, 2.25 mL, 1.5 mmol, 2.1 equiv). The reaction vessel was sealed and heated to 45 °C for 2 h. The volatile materials were removed *in vacuo*, and the light yellow residue was extracted with hexanes (5 × 5 mL). The combined extracts were filtered through a plug of Celite to give a colorless filtrate. The filtrate was concentrated to 15 mL and cooled to −40 °C. Colorless blocks were isolated (260 mg, 71% yield). ^{1}H NMR (400 MHz, C$_6$D$_6$): δ 1.59 (6 H, d, J = 5.8 Hz, PMe$_2$), 1.44 (9 H, d, J = 5.7 Hz, PMe$_3$), 1.36 (3 H, s, ring Me), 1.35 (3 H, s, ring Me), 1.08 (6 H, d, J = 9.0 Hz, PMe$_2$), 1.07 (6 H, d, J = 7.6 Hz, PMe$_2$), 0.55 (2 H, d, J = 7.2, 14.4 Hz, CH$_2$ SiP$_3$), 0.51 (2 H, d, J = 9.5 Hz, CH$_2$ SiP$_3$), 0.26 (2 H, dd, J = 6.2, 14.4 Hz, CH$_2$ SiP$_3$), 0.03 (2 H, dm, J = 9.1 Hz, ring CH$_2$), 0.00 (2 H, dm, J = 9.1 Hz, ring CH$_2$), −0.08 (3 H, s, Si−Me). ^{31}P{^{1}H}NMR (162 MHz, C$_6$D$_6$): δ 1.13 (dt, J = 315, 29 Hz, PMe$_2$), −4.20 (dt, J = 315, 28 Hz, PMe$_3$), −12.2 (dd, J = 28, 29 Hz, PMe$_2$). ^{13}C{^{1}H} NMR (100 MHz, C$_6$D$_6$) δ 48.5 (s, C$_q$), 37.5 (s, ring Me), 36.4 (s, ring Me), 29.8 (m, PMe$_2$), 23.8 (m, PMe$_2$), 23.6 (m, PMe$_3$), 21.5 (m, PMe$_2$), 19.9 (m, CH$_2$ SiP$_3$), 18.2 (m, CH$_2$ SiP$_3$), −0.7 (pseudo q, "J" = 5.3 Hz, Si−Me), −0.8 (dm, J = 52 Hz, ring CH$_2$). IR (KBr, cm^{-1}): 2971 (s), 2962 (s), 2924 (s), 2902 (s), 2881 (s), 2860 (s), 1468 (w), 1425 (m), 1416 (m), 1356 (m), 1338 (w), 1286 (m), 1275 (m), 1248 (m), 1095 (m), 1076 (m), 1028 (w), 1003 (m), 947 (m), 928 (s), 904 (s), 847 (m), 829 (s), 796 (m), 754 (s), 742 (s), 712 (m), 710 (m), 685 (s), 656 (m), 633 (m), 588 (w). MS (EI): m/z envelope centered at 440 (M$^+$ − PMe$_3$), 425 (M$^+$ − PMe$_3$ − Me). Anal. Calcd for C$_{18}$H$_{46}$P$_4$RuSi: C, 41.93; H, 8.99. Found: C, 42.30; H, 9.33.

(SiP$_3$)(PMe$_3$)Ru(CD$_2$CMe$_2$CH$_2$) (1-d_2). To a solution of (SiP$_3$)-(PMe$_3$)RuCl$_2$ (3) (95 mg, 0.18 mmol) in THF (10 mL) in a 30-mL glass bomb was added a Et$_2$O solution of Me$_3$CCD$_2$MgBr (0.23 M, 1.7 mL, 0.39 mmol, 2.2 equiv). The reaction vessel was sealed and heated to 45 °C for 2 h. The volatile materials were removed *in vacuo*, and the dark yellow residue was extracted with hexanes (5 × 5 mL). The combined extracts were filtered through a plug of Celite to give a colorless filtrate. The filtrate was concentrated to 15 mL and cooled to −20 °C. Colorless blocks were isolated (55 mg, 59% yield). ^{1}H NMR (400 MHz, C$_6$D$_6$): identical with that of 1, except integration of the δ 0.03 and 0.00 resonances gives 58% of the natural abundance value. ^{2}H{^{1}H} NMR (61.4 MHz, C$_6$H$_6$): δ 0.05 (br). MS (EI): m/z envelope centered at 442 (M$^+$ − PMe$_3$).

(SiP$_3$)(PMe$_3$)Ru(CH$_2$SiMe$_2$CH$_2$) (2). To a room temperature THF solution of (SiP$_3$)(PMe$_3$)RuCl$_2$ (15 mL, 243 mg, 0.47 mmol) in a 100-mL glass bomb was added a solution of Me$_3$SiCH$_2$MgCl in Et$_2$O (1.0 M, 1.0 mL, 1.0 mmol, 2.1 equiv). The reaction vessel was sealed and heated to 45 °C for 2 h. After the volatile materials were removed *in vacuo,* the colorless residue was extracted with pentane (5 × 3 mL). The combined extracts were filtered through a plug of Celite to give a colorless filtrate, which was concentrated (ca. 7 mL) and cooled (−40 °C, 12 h). Colorless blocks were isolated (194 mg, 78% yield). ^{1}H NMR (400 MHz, C$_6$D$_6$): δ 1.50 (6 H, d, J = 6.8 Hz, PMe$_2$), 1.35 (9 H, dd, J = 6.4, 1.1 Hz, PMe$_3$), 1.17 (6 H, d, J = 5.7 Hz, PMe$_2$), 1.04 (6 H, d, J = 4.3 Hz, ring Me (accidentally equivalent)), 0.47 (2 H, dd, J = 14.4, 7.5 Hz, SiP$_3$ CH$_2$), 0.46 (2 H, d, J = 7.5 Hz, SiP$_3$ CH$_2$), 0.22 (2 H, dd, J = 14.4, 7.8 Hz, SiP$_3$ CH$_2$), −0.08 (3 H, s, Si−Me), −1.22 (2 H, dt, J = 9.7, 12.7 Hz, ring CH$_2$), −1.37 (2 H, dt, J = 9.3, 12.6 Hz, ring CH$_2$). ^{31}P{^{1}H} NMR (162 MHz, C$_6$D$_6$): δ 1.70 (dt, J = 299, 30 Hz, PMe$_2$), −6.76 (dt, J = 299, 30 Hz, PMe$_3$), −12.2 (dd, J = 30, 30 Hz, PMe$_2$). ^{13}C{^{1}H} NMR (100 MHz, C$_6$D$_6$) δ 29.5 (m, PMe$_2$), 22.2 (m, PMe$_2$), 22.7 (m, PMe$_3$), 20.8 (dd, J = 16.6, 3.0 Hz, PMe$_2$), 19.2 (m, SiP$_3$ CH$_2$), 17.1 (m, SiP$_3$ CH$_2$), 10.6 (t, J = 3.0 Hz, ring Me), 9.4 (s, ring Me), −0.5 (pseudo q, "J" = 8.6 Hz, Si−Me), −29.2 (dm, J = 38 Hz, ring CH$_2$). IR (KBr, cm^{-1}): 2958 (s), 2920 (s), 2908 (s), 2883 (s), 2866 (s), 1421 (w), 1369 (m), 1288 (w), 1277 (w), 1250 (w), 1095 (m), 1076 (m), 1028 (w), 1005 (m), 949 (m), 928 (s), 905 (s), 876 (m), 862 (m), 829 (m), 796 (m), 752 (s), 701 (m), 688 (s), 634 (m), 606 (w), 455 (w). MS (EI): m/z 450 (M$^+$

− PMe$_3$), 441 (M$^+$ − PMe$_3$ − Me). Anal. Calcd for C$_{18}$H$_{46}$P$_4$RuSi: C, 38.40; H, 8.72. Found: C, 38.65; H, 8.91.

(SiP$_3$)Ru(Me)(η^3-CH$_2$CMeCH$_2$) (4). A toluene solution of 1 (20 mL, 144 mg, 0.28 mmol) in a glass bomb was heated (75 °C, 16 h). The volatile materials were removed *in vacuo* to yield 4 as a colorless solid (115 mg, 93% yield). Recrystallization from (Me$_3$Si)$_2$O (36 mg, 5 mL, 42% recovery) may be performed but usually is not necessary. ^{1}H NMR (400 MHz, C$_6$D$_6$; assignments were aided by the use of C−H correlation and NOESY experiments): 4$_{endo}$ δ 2.24 (2 H, d, J_{P-H} = 4.7 Hz, *anti*), 2.07 (3 H, s, Me allyl), 1.49 (2 H, dd, J_{P-H} = 4.2, 16.3 Hz, *syn*), 1.35 (6 H, d, J = 7.3 Hz, PMe$_2$), 1.17 (6 H, d, J = 7.3 Hz, PMe$_2$), 0.85 (6 H, d, J = 5.3 Hz, PMe$_2$), 0.56 (2 H, dd, J = 8.5, 14.6 Hz, CH$_2$ SiP$_3$), 0.39 (2 H, dd, J = 7.8, 14.6 Hz, CH$_2$ SiP$_3$), 0.31 (2 H, d, J = 9.1 Hz, CH$_2$ SiP$_3$), −0.03 (3 H, s, Si−Me), −0.64 (3 H, dt, J = 1.9, 9.4 Hz, Ru−Me); 4$_{exo}$ δ 2.63 (2 H, br s, *anti*), 2.13 (3 H, s, Me allyl), 1.73 (2 H, br m, *syn*), 1.34 (br, obscured in ^{31}P coupled spectrum, PMe$_2$), 1.31 (6H, d, J = 7.8 Hz, PMe$_2$), 0.92 (6H, d, J = 5.2 Hz, PMe$_2$), 0.49 (dm, obscured in ^{31}P coupled spectrum, J_{H-H} = 14.3 Hz, CH$_2$ SiP$_3$), 0.39 (dm, obscured in ^{31}P coupled spectrum, J_{H-H} = 14.3 Hz, CH$_2$ SiP$_3$), 0.22 (2H, d, J = 10.1 Hz, CH$_2$ SiP$_3$), −0.07 (3 H, s, Si−Me), −0.61 (obscured in ^{31}P coupled spectrum, Ru−Me). ^{31}P{^{1}H} NMR (162 MHz, C$_6$D$_6$): 4$_{endo}$ δ 8.91 (d, J = 23 Hz), −7.73 (t, J = 23 Hz); 4$_{exo}$ δ 8.23 (d, J = 27), −7.10 (t, J = 27 Hz). ^{13}C{^{1}H} NMR (100 MHz, toluene-d_8): 4$_{endo}$ δ 112.7 (s, C$_q$), 36.9 (m, CH$_2$ allyl), 28.3 (dd, J = 10.6, 14 .4 Hz, PMe$_2$), 25.4 (s, Me allyl), 20.2 (ddd, J = 2.0, 3.8, 12.5 Hz, PMe$_2$), 19.9 (ddd, J = 4.1, 8.4, 21.4 Hz, PMe$_2$), 17.6 (dd, J = 3.0, 3.0 Hz, CH$_2$ SiP$_3$), 16.0 (dd, J = 2.0, 2.5 Hz, CH$_2$ SiP$_3$), 0.5 (pseudo q, "J" = 6.2 Hz, Si−Me), −3.0 (dt, J = 60.9, 12.5 Hz, Ru−Me); 4$_{exo}$ δ 113.6 (s, C$_q$), 48.6 (m, CH$_2$ allyl), 30.15 (d, J = 7.5 Hz, PMe$_2$), 28.5 (s, Me allyl), 24.7 (dt, J = 8.5, 2.0 Hz, PMe$_2$), 21.2 (dm, J = 24.8 Hz, PMe$_2$), 17.4 (m, CH$_2$ SiP$_3$), 14.3 (m, CH$_2$ SiP$_3$), 8.5 (dt, J = 72.5, 13.8 Hz, Ru−Me), 0.3 (m, Si−Me). IR (KBr, cm^{-1}): 3055 (w), 3022 (w), 2966 (s), 2922 (s), 2904 (s), 2883 (s), 2870 (s), 2819 (m), 1421 (m), 1412 (m), 1367 (m), 1286 (m), 1273 (m), 1246 (m), 1161 (w), 1092 (s), 1074 (s), 1028 (m), 1005 (m), 928 (s), 904 (s), 748 (s), 712 (m), 688 (s), 633 (m), 590 (s), 559 (m), 459 (w), 411 (w). MS (EI): m/z 440 (M$^+$), 425 (M$^+$ − Me). Anal. Calcd for C$_{15}$H$_{37}$P$_3$RuSi: C, 40.99; H, 8.48. Found: C, 40.81; H, 8.69.

Thermolysis of 1-d_2. An NMR tube was loaded with a solution of 1-d_2 (16 mg, 0.031 mmol) in C$_6$D$_6$. The contents of the tube were degassed by a freeze−pump−thaw cycle, and the tube was flame sealed. The solution was heated at 75 °C for 8 h. ^{1}H NMR (400 MHz, C$_6$D$_6$): identical with the spectrum for 4, except that the allyl *syn* and *anti* resonances integrated to 55% of the natural abundance values on average. There was also a small amount of complex 1-d_2 observed in this spectrum. ^{2}H{^{1}H} NMR (61.4 MHz, C$_6$H$_6$): δ 2.65 (s, *exo anti*), 2.25 (s, *endo anti*), 1.75 (d, J = 2 Hz, *exo syn*), 1.5 (d, J = 2 Hz, *endo anti*), 0.05 (br, residual 1-d_2). No ^{2}H resonances were observed at −0.6 ppm.

(SiP$_3$)(PMe$_3$)Ru(CH$_3$)$_2$ (5). A THF solution of CH$_3$MgCl (3.0 M, 1.50 mL, 4.5 mmol, 2.3 equiv) was added to a solution of 3 (1.03 g, 2.0 mmol) in 75 mL of C$_6$H$_6$ by syringe. The reaction mixture was stirred until the change in color from yellow to colorless was complete (ca. 15 min). The volatile materials were removed *in vacuo*, and the light yellow residue was extracted with hexanes (1 × 50 mL, 2 × 10 mL). The combined extracts were filtered through a plug of Celite to give a colorless filtrate. The filtrate was concentrated (15 mL) and cooled (−40 °C, 12 h). Colorless blocks were isolated (598 mg, 63% yield). ^{1}H NMR (400 MHz, C$_6$D$_6$): δ 1.25 (6 H, d, J = 6.8 Hz, PMe$_2$), 1.23 (6 H, d, J = 5.4 Hz, PMe$_2$), 1.15 (9 H, dd, J = 6.2, 1.1 Hz, PMe$_3$), 1.12 (6 H, d, J = 4.0 Hz, PMe$_2$), 0.48 (2 H, dd, J = 7.6, 14.4 Hz, SiP$_3$ CH$_2$), 0.40 (2 H, d, J = 8.4 Hz, SiP$_3$ CH$_2$), 0.38 (2 H, d, J = 8.4, 14.4 Hz, SiP$_3$ CH$_2$), −0.61 (3 H, s, Si−Me), −0.30 (6 H, m, Ru−CH$_3$). ^{31}P{^{1}H} NMR (162 MHz, C$_6$D$_6$): δ 7.50 (dt, J = 322, 28 Hz, PMe$_2$), 0.96 (dt, J = 321, 27 Hz, PMe$_3$), −5.93 (dd, J = 28, 27 Hz, PMe$_2$). ^{13}C{^{1}H} NMR (100 MHz, C$_6$D$_6$) δ 29.2 (m, PMe$_2$), 21.6 (m, PMe$_3$), 19.2 (m, SiP$_3$ CH$_2$), 19.1 (m, PMe$_2$), 18.1 (m, PMe$_2$), 15.6 (m, SiP$_3$ CH$_2$), 0.6 (pseudo q, "J" = 6 Hz, Si−Me), −6.7 (d"q", J = 65, 13 Hz, Ru−CH$_3$). IR (KBr, cm^{-1}): 2968 (s), 2906 (s), 2883 (s), 2873 (s) 2856 (m), 2836 (m), 2791 (m), 1473 (m), 1444 (m), 1431 (s), 1404 (m), 1379 (m), 1367 (m), 1298 (w), 1286 (m), 1274 (m), 1245 (w), 1099 (m), 1059 (m), 1070 (m), 1007 (w), 953 (m), 929 (vs), 904 (vs),

846 (m), 831 (s), 796 (m), 752 (s), 708 (m), 688 (m), 673 (m), 663 (m), 634 (m), 594 (w). MS (FAB+, sulfolane): *m/z* envelope centered at 476.1 (M^+), 461 ($M^+ -$ Me). Anal. Calcd for $C_{15}H_{42}P_4RuSi$: C, 37.89; H, 8.90. Found: C, 38.19; H, 8.65.

Preparation of 4 from 5. To a solution of **5** in Et_2O (40 mL, 51 mg, 0.098 mmol) cooled at -78 °C was added a solution of HCl in Et_2O (0.019 M, 5.1 mL, 0.098 mmol, 1.0 equiv) over 2 h with stirring. The volatile materials were removed *in vacuo*. The residue was examined by ^1H NMR and was found to be composed of a mixture (ca. 4:1) of $(SiP_3)(PMe_3)Ru(Me)(Cl)$ (**6**) and **3**. A toluene solution of the residue (ca. 5 mL) was layered with pentane (ca. 2 mL) and cooled to -40 °C. Crystals (11 mg) from this solution were found to be enriched in **3** (ca. 2:1 **6:3**). Evaporation of the mother liquor yielded a clean sample of **6** (16 mg, 0.030 mmol, 31% yield). This sample was dissolved in C_6D_6 along with an internal standard (p-$(MeO)_2C_6H_4$) and treated with CH_2=$CH(Me)CH_2MgBr$ in Et_2O (0.29 M, 0.11 mL, 0.032 mmol, 1 equiv). The reaction was monitored over the course of 1 day at room temperature by ^1H and $^{31}P\{^1H\}$ NMR. The overall conversion from **6** to **4** was found to be 96% on the basis of integration versus the internal standard.

Spectroscopic Data for $(SiP_3)(PMe_3)Ru(Me)(Cl)$ (6). ^1H NMR (400 MHz, C_6D_6): δ 1.64 (3 H, d, $J = 7.7$ Hz, PMe), 1.57 (3 H, d, $J = 6.3$ Hz, PMe), 1.29 (9 H, d, $J = 5.4$ Hz, PMe_3), 1.26 (3 H, d, $J = 6.8$ Hz, PMe), 1.08 (3 H, d, $J = 5.9$ Hz, PMe), 1.06 (3 H, d, $J = 6.8$ Hz, PMe), 0.92 (3 H, d, $J = 7.3$ Hz, PMe), 0.34$-$0.5 (2 H, m, SiP_3 CH_2), 0.2$-$0.3 (7 H, m, SiP_3 CH_2 + Ru$-$$CH_3$), 0.24 (3 H, s, Si$-$$CH_3$). $^{31}P\{^1H\}$ NMR (162 MHz, C_6D_6): δ 22.9 (ddd, $J = 24, 31, 40$ Hz), 5.8 (ddd, $J = 25, 44, 324$ Hz), -7.3 (ddd, $J = 28, 30, 32$ Hz), -9.8 (ddd, J = 23, 23, 23 Hz).

$(SiP_3)Ru(TMM)$ (7). A solution of **4** in toluene (100 mg, 0.23 mmol, 20 mL) was heated at 135 °C for 3 days in a sealed glass bomb. The reaction progress was followed by examining aliquots by $^{31}P\{^1H\}$ NMR spectroscopy. The reaction mixture was evaporated to dryness under vacuum. The residue was sublimed (100 °C, 0.1 torr) to yield a colorless solid (28 mg, 0.066 mmol, 29%). ^1H NMR (400 MHz, C_6D_6): δ 1.29 (6 H, m, TMM), 1.19 (18 H, vt, $J = 3.2$ Hz, PMe_2), 0.52 (6 H, pseudo q, "J" = 2.8 Hz, SiP_3 CH_2), 0.01 (3 H, q, $J = 0.8$ Hz, Si$-$Me). $^{31}P\{^1H\}$ NMR (162 MHz, C_6D_6): δ 7.99 (s). $^{13}C\{^1H\}$ NMR (100 MHz, C_6D_6): δ 107.5 (s, C_q), 37.5 (m, TMM CH_2), 26.9 (m, PMe_2), 16.1 (m, SiP_3 CH_2), 0.0 (m, Si$-$Me). IR (KBr, cm^{-1}): 2970 (s), 2907 (s), 2881 (s), 1429 (m), 1368 (w), 1288 (m), 1275 (m), 1247 (m), 1090 (m), 1073 (m), 931 (s), 714 (m), 670 (w), 635 (m). Anal. Calcd for $C_{13}H_{33}P_3RuSi$: C, 39.71; H, 7.85. Found: C, 39.52; H, 7.88.

Crystal Structure Determination of 1. Colorless block-like crystals of **1** were obtained by crystallization from hexanes at -35 °C. Data were collected on an Enraf-Nonius CAD-4 diffractometer at -92 °C. The final cell parameters and specific data collection parameters for this data set are given in the Supporting Information. The 1930 raw intensity data were converted to structure factor amplitudes by correction for scan speed, background, and Lorentz polarization effects. Space group *Pnma* was confirmed by successful refinement. Inspection of the azimuthal scan data showed a variation of $I_{min}/I_{max} = 0.85$. An empirical absorption correction based on the observed variation was applied to the data. The structure was solved by Patterson methods and refined via standard least-squares and Fourier techniques.

The molecule was found to lie on a crystallographic mirror plane with the tripodal ligand disordered about the mirror plane. The disorder was modeled as two sets of half-occupancy carbon atom positions corresponding to the two twist conformations of the tripodal ligand. The hydrogen atom positions were not located in the difference map, nor were they calculated. The half-occupancy carbon atoms were refined isotropically; all of the other atoms were refined with anisotropic thermal parameters. Three reflections with abnormally large structure factors were given zero weight in the final refinement. The final residuals for 118 variables refined against the 1465 data for which $F^2 > 3\sigma(F^2)$ were $R = 7.8\%$, $R_w = 10.4\%$, and GOF = 5.23. The R value for all 1719 data was 8.9%. An ORTEP representation showing one conformation is shown in Figure 1. The positional parameters, anisotropic thermal parameters, and bond distances and angles are included in the Supporting Information.

Crystal Structure Determination of 7. Colorless block-like crystals of **7** were obtained by crystallization from hexanes at -35 °C. Data were collected on a Siemens SMART diffractometer at -88 °C. The final cell parameters and specific data collection parameters for this data set are given in the Supporting Information. Collection of a full hemisphere of reciprocal space was measured by using 20-s frames of width 0.3° in ω. The data were corrected for Lorentz and polarization effects. An additional correction for secondary absorption was applied (coefficient = 1.16702×10^{-6}). No decay correction was applied. Of the 7052 reflections collected, 3396 were unique; equivalent reflections were merged.

Data analysis was performed with a Siemens XPREP. The space group was determined to be $P2_1/n$ (No. 14) on the basis of the cell parameters and systematic absences. The structure was solved and refined with the teXsan software package using direct methods and expanded with Fourier techniques. The hydrogen atoms were located and their positions refined with isotropic thermal parameters ($B = 2.5$); all other atom positions were refined with anisotropic thermal parameters. The final cycle of full-matrix least-squares refinement was based on 2995 observed reflections ($I > 3\sigma(I)$) and 305 variable parameters and converged with unweighted and weighted agreement factors of $R = 0.028$ and $R_w = 0.039$. The weighting scheme was based on counting statistics and included a factor ($p = 0.025$) to downweight the intense reflections. The maximum and minimum peaks in the final Fourier difference map corresponded to 0.36 and -0.42 $e^-/Å^3$. The positional parameters, anisotropic thermal parameters, and bond distances and angles are included in the Supporting Information.

Supporting Information Available: ORTEP diagrams, crystal and data collection parameters, positional parameters, anisotropic thermal parameters, and intramolecular distances and angles for **1** and **7** and EXSY data for **4** (13 pages). See any current masthead page for ordering and Internet access instructions.

JA972131E